Biogeochemistry (2021) 156:279–292
https://doi.org/10.1007/s10533-021-00845-0

Temperature controls diel oscillation of the CO_2 concentration in a desert soil

Marie Spohn · **Stefan Holzheu**

Received: 2 May 2021 / Accepted: 24 August 2021 / Published online: 8 September 2021

Abstract The diel dynamic of the CO_2 concentration in soils in relation to temperature is not yet fully understood. Air temperature might control the soil CO_2 concentration due to thermal convective venting at sites experiencing large temperature differences between the atmosphere and the soil. Therefore, the objective of this study was to determine the soil CO_2 concentration and its temporal dynamic in a deep desert soil in relationship to soil and air temperature based on high frequency measurements. For this purpose, CO_2 concentration and temperature were measured in six soil depths (ranging from 15 to 185 cm) in a coarse-textured desert soil in the North of Chile every 60 min together with precipitation and air temperature for one year. The mean CO_2 concentration calculated across the whole measuring period increased linearly with soil depth from 463 ppm in 15 cm to 1542 ppm in 185 cm depth. We observed a strong diel oscillation of the CO_2 concentration that decreased with soil depth and a hysteretic relationship between the topsoil CO_2 concentration and both air and soil temperature. The Rayleigh-Darcy number calculated for different times indicates that thermal convective venting of the soil occurred during the night and in the early morning. A small precipitation event (4 mm) increased the CO_2 concentrations in 15, 30, and 50 cm depths for several days but did not alter the amplitude of the diel oscillation of the CO_2 concentration. The diel oscillation of the CO_2 concentration and the hysteretic relationship between soil CO_2 concentration and air temperature were likely caused by thermal convection, leading to transport of CO_2-rich air from the soil to the atmosphere at night. In conclusion, our results indicate that the soil CO_2 concentration can be largely controlled by convection caused by temperature differences, and not only by diffusion. The results have important implications as they provide further evidence that thermal convective venting contributes to gas exchange at sites experiencing large temperature differences between the atmosphere and the soil, which is relevant for soil chemical reactions.

Keywords Soil CO_2 concentration · Desert soil · Hysteresis · Diel oscillation · Soil depth · Precipitation

Responsible Editor: Sharon A. Billings.

Supplementary Information The online version contains supplementary material available at https://doi.org/10.1007/s10533-021-00845-0.

M. Spohn (✉) · S. Holzheu
Bayreuth Center of Ecology and Environmental Research (BayCEER), University of Bayreuth, Bayreuth, Germany
e-mail: marie.spohn@slu.se

M. Spohn
Department of Soil and Environment, Biogeochemistry of Forest Soils, Swedish University of Agricultural Sciences, Uppsala, Sweden

Introduction

The CO_2 concentration in soils is usually much higher than in the atmosphere (Amundson and Davidson 1990) and can be very dynamic (Riveros-Iregui et al. 2007). However, the diel dynamic of the CO_2 concentration in soils in relation to temperature is not yet fully understood (Philipps et al. 2011). The soil CO_2 concentration results from the production and transport of CO_2. CO_2 is produced in soils by microbial and root respiration (Schimel et al. 2001) as well as by the dissolution of carbonates in calcareous soils (Ramnarine et al. 2012). Only at a few, exceptional sites is CO_2 derived from geothermal sources (Kämpf et al. 2013). The production of CO_2 by soil microorganisms depends on soil temperature and moisture (Wood et al. 1993; Moyano et al. 2013; Schimel 2018). The production of CO_2 in soil by plant roots depends additionally on solar radiation (Carbone and Trumbore 2007). Traditionally, it was believed that the transport of CO_2 from the soil to the atmosphere is driven only by diffusion (Amundson and Davidson 1990). However, recent studies demonstrated that also advection, i.e., movement of CO_2 through movement of air, contributes to the transport of CO_2 from the soil to the atmosphere (Maier et al. 2012; Rey 2015; Moya et al. 2019). Advective movement of air in soil pores and from the soil to the atmosphere can be caused by small turbulence-induced pressure fluctuations which can be induced by wind (Takles et al. 2004; Flechard et al. 2007; Maier et al. 2012; Sánchez-Cañete et al. 2013; Moya et al. 2019; Laemmel et al. 2019). In addition, thermal differences between soil and air can cause movement of air from soil pores to the atmosphere, called thermal convection, free convection, or thermal convective venting (TCV) (Rose and Guo 1995; Ganot et al. 2014; Roland et al. 2015; Rey et al. 2015; Levintal et al. 2017; Laemmel et al. 2019). TCV likely occurs mostly in (semi-)desert ecosystems (Weisbrod et al. 2009; Ganot et al. 2014; Levintal et al. 2017) because of the large differences between soil and air temperature at night (Noy-Meir 1973; Nachshon et al. 2011). However, there are so far only very few studies that explored TCV under field conditions.

TCV is caused by a higher temperature of the soil than of the air in combination with high soil permeability. The temperature difference between soil and air creates unstable conditions in the soil profile as warm, less dense gas underlies cold, denser gas (Nachshon et al. 2011; Ganot et al. 2014). If the buoyancy forces overcome the impeding viscous forces, convective gas motion within the soil profile takes place. Whether thermal convective venting (TCV) occurs in homogeneous porous media can be assessed based on the Rayleigh-Darcy number (*Ra*). *Ra* is a dimensionless number that shows the ratio of buoyant and viscous forces.

$$Ra = \frac{g\beta\Delta TkH}{v\alpha_s} \quad (1)$$

where g is the gravitational acceleration, β is the volumetric thermal expansion coefficient, ΔT is the temperature difference between the bottom and the top of the soil, k is the permeability, H is the soil depth, v is the kinematic viscosity of the fluid, and α_s is the thermal diffusivity of the soil (Nield and Bejan 2013). Equation 1 shows that TCV is likely to occur in deep soils and in highly permeable soils, when the soil is warmer than the air. An increase in both ΔT and H will increase the buoyancy forces that promote heat convection, and hence *Ra*. Increasing H will decrease the thermal gradient, and thus the proportion of heat transferred by conduction, which increases the buoyancy forces. Under the assumption that (i) soil is homogeneous and isotropic, (ii) Darcy's law and the Boussinesq approximation are valid (Nield and Bejan 2013), and (iii) air is the only mobile fluid in the soil, the minimal *Ra* value that is needed for TCV to occur is approximately 27 (Ribando and Torrance 1976; Tan et al. 2003).

During recent years, new CO_2 sensors have made it possible to measure CO_2 concentrations at high frequency, which gives rise to the description of hourly and sub-hourly changes in the soil CO_2 concentration (Jassal et al. 2005; Riveros-Iregui et al. 2007; Sánchez-Cañete et al. 2013; Zhang et al. 2015; Moya et al. 2019). Based on these high frequency measurements of the soil CO_2 concentration, a hysteresis loop was found when plotting the CO_2 concentration as a function of the soil temperature in a high-altitudinal, semi-arid forest soil (Riveros-Iregui et al. 2007). A very similar relationship between soil CO_2 concentration and soil temperature was also observed in a temperate pine plantation (Zhang et al. 2015) and Mediterranean cropland soils (Min et al. 2020). In addition, several authors reported a hysteresis loop when plotting the CO_2 efflux as a

function of soil temperature (Parkin and Kaspar 2003; Gaumont-Guay et al. 2006; Ruehr et al. 2010; Jia et al. 2013; Wang et al. 2014; Song et al. 2015; Zhang et al. 2015).

The reasons for the hysteresis observed between soil temperature and soil CO_2 concentration or CO_2 efflux have been debated intensively. Initially, the phenomenon has been explained by changes in soil CO_2 production by biota that depend on soil temperature (Riveros-Iregui et al. 2007). Later, Ruehr et al. (2010) pointed out that the hysteretic relationship between soil temperature and CO_2 observed in a forest soil indicated an unusually high temperature sensitivity of soil respiration ($Q_{10} > 150$), making it rather unlikely that changes in CO_2 are caused by temperature-dependent biotic activity. Philipps et al. (2011) showed based on a model that the hysteresis can result from heat and CO_2 transport processes in soil alone without changes in biological CO_2 production. In the following years, several authors discussed possible biotic and the abiotic components of the hysteresis (Wang et al. 2014; Song et al. 2015; Zhang et al. 2015). However, despite the fact that temporal dynamics of CO_2 are more closely related to the air temperature than to the soil temperature in some ecosystems (Parking and Kasper 2003), there is no study that analyzed and discussed changes in air temperature as the reason for the hysteresis, to our knowledge.

The objective of this study was to determine the soil CO_2 concentration and explore its temporal dynamic in relation to soil and air temperature in a deeply weathered desert soil. We hypothesized that the CO_2 concentration undergoes diel changes due to the strong changes in air temperature and shows a hysteretic relationship both with soil and air temperature.

Material and methods

Study site

The study site (for a photo see Supplementary Information) is located in the Coastal Cordillera of Chile in the reserve Santa Gracia close to the city La Serena, at 615 m a.s.l. (− 29.759769°, − 70.457333°). The mean annual temperature is 16.1 °C and mean annual precipitation is 87 mm per year (Oeser et al. 2018). The soil is locates on a hillslope (15° slope angle), and many coarse stones are visible on the surface (5% cover). The vegetation is sparse (~ 10% cover) and dominated by *Proustia cuneifolia*, *Cordia decandra* and *Adesmia* spp. The parent material of the soil is granodiorite (Oeser et al. 2018). The soil is a Cambisol (according to the world reference base for soil resources (WRB)) and consists of a 30 cm deep A horizon overlying a B horizon, ranging from 30 to 80 cm depth, a B-Cw horizon ranging from 80 to 120 cm, and below 120 cm until > 200 cm a Cw horizon. The bulk density varies between 1.42 and 1.66 g cm^{-3} (Bernhard et al. 2018). The root density is low; 3–5 fine roots per dm^2 in the A horizon, and 1–2 fine roots per dm^2 in the B horizon. In the B-Cw and Cw horizon, roots are only present in fractures. The bedrock is deeply weathered, which is typical for the Coastal Cordillera of Chile (Vázquez et al. 2016), and particularly the upper meters of the soil and saprolite contain many fractures (Krone et al. 2021). More information about the soil at the study site can be found in Bernhard et al. (2018), Oeser et al. (2018), Brucker and Spohn (2019), and Krone et al. (2021).

Sampling and study design

In March 2019, we excavated a 2 m deep soil profile at the site, and the excavated material was stored in different heaps according to the depth it was taken from. Soil samples were collected from the following depths: 0–5, 5–10, 10–20 cm, and further in 20 cm intervals until 200 cm soil depth (i.e. 20–40, 40–60 cm, etc.). Subsequently, we dug 25 cm long, flat, horizontal tunnels into the profile wall using a chisel at the following depths; 15, 30, 50, 90, 135, and 185 cm. In these tunnels, the temperature and the CO_2 sensors were placed. The tunnels were closed with the material that was removed when building the tunnels and, subsequently, the whole profile was closed by filling the material of the different soil depths increments into the soil pit in the right order. The temperature sensor (DS18B20) and the CO_2 sensor (R30, Sense Air) of one soil depth were controlled together by a self-built Arduino clone board with flash storage and real time clock crystal (https://www.bayceer.uni-bayreuth.de/bayeos/en/sensor_net/gru/html.php?id_obj=145275). The two sensors of each soil depth and the corresponding Arduino board were powered by four lithium-ion batteries. The CO_2 sensors had been calibrated before deployment in the field

using gases with known CO_2 concentration in closed glass jars. The temperature and the CO_2 concentration were measured and logged every 60 min. Most sensors stopped measuring at the end of January 2020 when the battery charge got low. The sensors in soil depth 130 cm measured continuously over the whole year. Batteries of all sensors were changed on March 8, 2020, and subsequently, temperature as well as CO_2 concentration were measured and logged until May 5, 2020.

We also used data from the weather station (Campbell Scientific) installed at the study site (for details see Übernickel et al. (2020)). The weather station measures the air temperature 200 cm above the soil using a temperature sensor (HC2S3, Rotronic) and the precipitation using a tipping bucket rain gauge (ARG 100, Environmental Measurements Limited), at an interval of 60 min.

Soil chemical and physical analyses

One part of each soil sample was dried at 15 °C. Subsequently, the gravel content was determined by sieving (< 60 mm and > 2 mm). The texture of the < 2 mm fraction was determined using the standard soil pipette texture method according to Burt (2004) after destruction of organic matter using H_2O_2. The pH was measured in a soil:water ratio of 1:2.5 using a pH meter (pH 340, WTW GmbH, Weilheim, Germany) with a Sentix 81 electrode. A subsample of the fine earth fraction was dried at 105 °C and ground in a ball mill for the determination of the carbonate content and the total organic C (TOC) and total N (TN) content. TOC and TN were measured using an element analyzer (Vario Max Elementar, Hanau). The absence of carbonates was confirmed using 30% HCl.

In order to assess the amount of microbial biomass, we determined the DNA content in field moist samples. The samples were passed through a sieve (2 mm). DNA was extracted from 400 mg of field moist soil using a DNA extraction kit (FastDNA^{TM} SPIN Kit for Soil, MP Biomedicals) with small modifications as in Spohn et al. (2016). The DNA concentration was measured with the picogreen assay (Sandaa et al. 1998) using a kit (Quant-iT^{TM} PicoGreen® dsDNA Reagent, Life Technologies).

Data analysis and calculations

For the data analysis, the first six weeks after installation of the sensors were not considered because there might have been artifacts in the CO_2 concentration due to the settling of the soil in the soil pit. For the following period from May 1, 2019 until May 5, 2020, we calculated monthly means of temperature and CO_2 concentration across all measurements of one month (n = 720 or 744, and 696 in February), daily means across all 24 h of the day (n = 24), and hourly means for specific months across all days of the month (n = 30 or 31 and 29 in February). All data analyses were conducted in R (R Core Team 2018).

We calculated *Ra* according to Eq. 1, using the following values for the constants; g = 9.806 m s^{-2}, β = 3.41 × 10^{-3} °C^{-1}, ν = 1.53 × 10^{-5} m^2 s^{-1}. We computed α_s following Ganot et al. (2014) as

$$\alpha_s = \kappa_s \kappa_f^{-1} \alpha_f \quad (2)$$

where κ_s and κ_f are the thermal conductivities of the soil and the fluid (i.e., the air), and α_f is the thermal diffusivity of the fluid, using the following values: κ_f = 2.58 × 10^{-2} W m^{-1} °C^{-1}, α_f = 2.16 × 10^{-5} m^2 s^{-1}, κ_s = 0.27 W m^{-1} °C^{-1} (Ganot et al. 2014). We considered ΔT as the difference between the soil temperature in a given soil depth (specified in the Results section) and the air temperature above the soil, following Levintal et al. (2017). We used different estimates of the permeability (k) based on data about the permeability for soil, sand as well as gravel and sand mixtures (Ganot et al. 2014; Côté et al. 2011; Bear, 2013), as specified in the Results section.

Results

Soil physical and chemical properties

The soil had a high content of fragments of weathered saprolite > 2 mm (called gravel in the following) and a sandy texture (Table 1). In the 100–200 cm depth, the gravel content ranged around 50% of the soil mass. The gravel content and the sand content increased with increasing soil depth, while the silt and clay content decreased with increasing depth (Table 1). The pH decreased from pH 8.3 in the upper 5 cm to pH 6.1 in 180–200 cm depth (Table 1). The soil was completely

Table 1 Soil properties, including gravel content (mineral particles > 2 mm), soil texture (of the fraction < 2 mm), pH determined in water, total organic carbon (TOC), total nitrogen (TN), and soil DNA content, b.d.l. stands for below detection limit

Soil depth (cm)	Gravel (%)	Soil texture			pH_{H2O}	TOC (g kg^{-1})	TN (g kg^{-1})	Molar TOC:TN ratio	DNA (mg kg^{-1})
		Sand (%)	Silt (%)	Clay (%)					
0–5	13.6	72.0	22.8	5.2	8.3	12.37	0.93	10.6	5.1
5–10	10.7	72.5	21.3	6.1	8.6	10.34	0.81	10.2	14.0
10–20	19.8	68.8	20.5	10.6	8.4	8.03	0.66	9.8	65.5
20–40	30.4	71.1	15.8	13.1	8.2	5.61	0.40	11.2	25.6
40–60	50.0	79.9	11.0	9.1	8.1	2.40	0.19	9.9	5.0
60–80	46.3	82.3	11.2	6.4	7.9	1.55	0.12	10.5	3.35
80–100	54.4	85.1	10.0	4.9	7.8	1.41	0.10	11.1	2.15
100–120	44.5	89.1	8.0	2.9	7.7	1.02	b.d.l	–	1.49
120–140	48.9	89.0	8.7	2.3	7.6	0.87	b.d.l	–	1.31
140–160	46.6	87.1	8.6	4.3	7.2	1.14	0.09	9.7	1.23
160–180	48.1	87.9	8.8	3.3	6.3	0.99	0.07	10.6	1.38
180–200	54.8	90.5	7.6	1.9	6.1	0.92	b.d.l	–	1.14

carbonate free. Both TOC and TN concentrations were highest in the upper 5 cm and decreased strongly with increasing soil depth. The TOC concentration decreased by 80% from the upper 5 cm to 40–60 cm depth. The DNA concentration was much higher in the upper 60 cm than in the lower part of the soil profile. The molar TOC:TN ratio ranged between 9.7 and 11.1 and showed no trend with soil depth. In contrast to the TOC concentration, the DNA concentration was highest from 10 to 20 cm depth (Table 1).

Annual variation of temperature and CO_2 concentrations

The mean air temperature ranged between a monthly mean of 9.2 °C in July and 20.2 °C in December. There were a few small precipitation events between May 30 and mid-July (Fig. 1). During these events, the precipitation rate did not exceed 3–4 mm per hour. The first of these events occurred on May 29.

The mean monthly soil temperature in 15 cm depth was 13.5 °C in July and 27.1 °C in December. The variability in the daily means of soil temperature decreased with increasing soil depth (Fig. 2a). Between May and August the daily mean soil temperature was higher in the subsoil than in the topsoil and increased with increasing depth. In contrast, from late October to April the temperature declined with increasing depth (Fig. 2a).

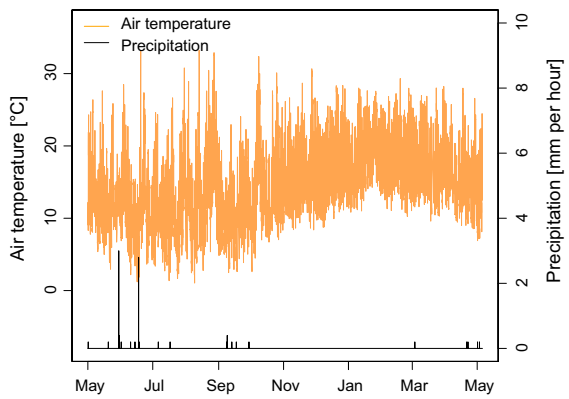

Fig. 1 Air temperature and precipitation at the study site from May 2019 until May 2020

The CO_2 concentration increased with depth from 15 to 185 cm soil depth throughout the year (Fig. 2b). The mean of the CO_2 concentration for the period from May 1, 2019 until May 5, 2020 was 463 ppm in 15 cm depth, 533 ppm in 30 cm depth, 712 ppm in 50 cm depth, and 696 ppm in 90 cm depth, 1032 ppm in 130 cm depth, and 1578 ppm in 185 cm depth. The mean CO_2 concentrations of the six soil depths were positively correlated with soil depth ($R^2 = 0.93$, $p < 0.05$). The variability in the daily means of the

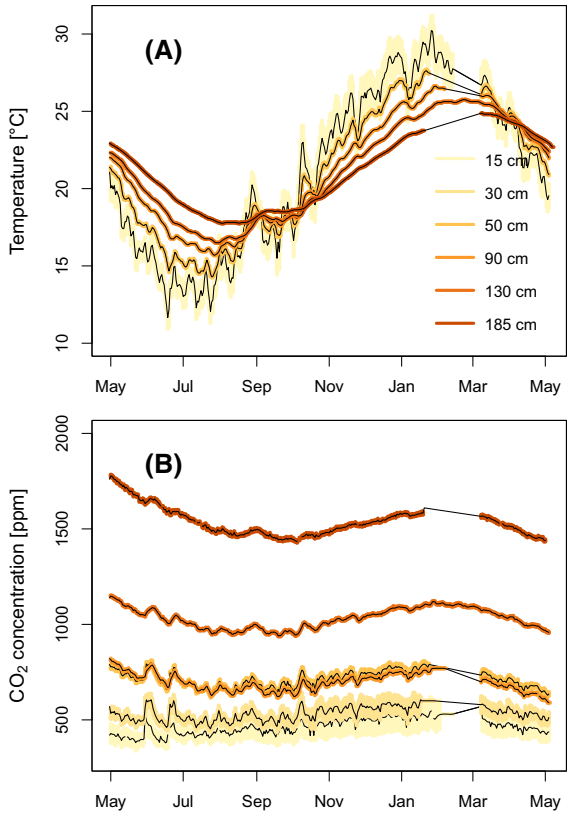

Fig. 2 Soil temperature (**a**) and soil CO_2 concentration (**b**) in six soil depths. Black lines show daily means and colored shades show daily standard deviations (n = 24)

CO_2 concentration decreased with increasing soil depth (Fig. 2b).

Diel variation of soil CO_2

The soil CO_2 concentration in the topsoil changed considerably over the day (Fig. 3). In July, the mean CO_2 concentration in 15 cm depth, calculated across all days of the month, increased by 95 ppm between 10:00 h and 18:00 h. In December, the CO_2 concentration in 15 cm depth changed more strongly than in July over the course of the day, namely by 211 ppm, from 418 ppm at 9:00 h to 629 ppm at 17:00 h (Fig. 3a). In December, in 30 cm depth, the maximum CO_2 concentration was shifted by some hours in comparison to 15 cm soil depth, and was observed at 23:00 h (Fig. 3b). In 50 cm soil depth, the maximum CO_2 concentration was time-shifted in comparison to 30 cm soil depth, and was observed at 2:00 h (Fig. 3c).

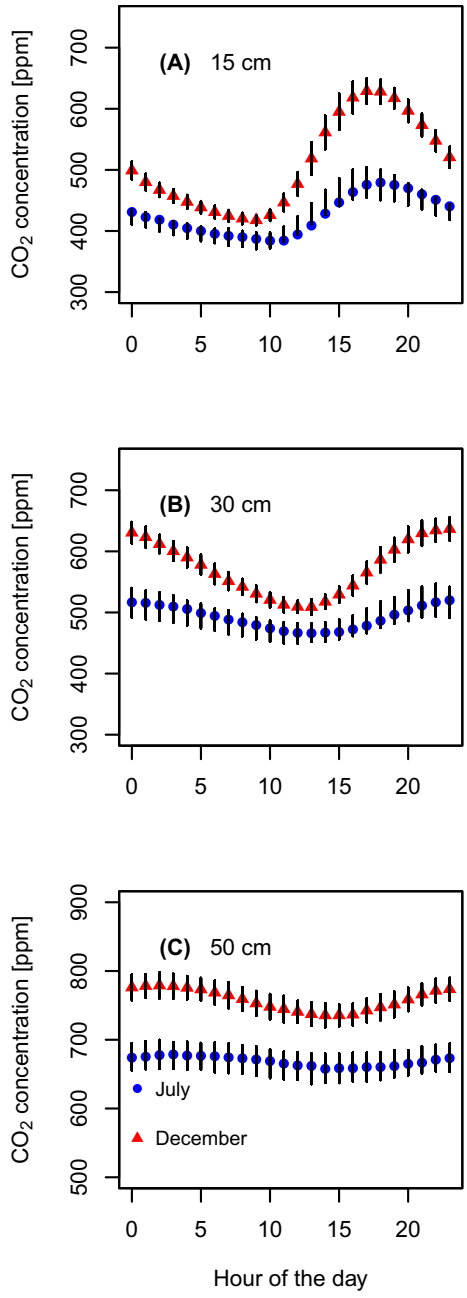

Fig. 3 CO_2 concentrations in 15 cm (**a**), 30 cm (**b**), and 50 cm (**c**) depth in July and December as a function of time of the day. Symbols indicate means, and arrows depict standard deviations calculated across all days of the two months in 2019 (n = 24)

Diel variation of temperature and *Ra*

Similar to the CO_2 concentration in the topsoil, the air temperature in the upper 15 cm varied strongly over the course of the day during all seasons. In July, the

mean air temperature, calculated across all days of the month, ranged from 3.6 °C at 9:00 h to 17.8 °C at 17:00 h. In December, the mean air temperature ranged from 11.0 °C at 7:00 h to 30.4 °C at 16:00 h (Fig. 3a). In contrast, the soil temperature changed little during the day, even in the uppermost 15 cm (Fig. 4b). In July, the mean soil temperature at 15 cm depth calculated across all days of the month, ranged from 12.5 °C at 13:00 h to 14.4 °C at 23:00 h. In December, the mean temperature at 15 cm soil depth ranged from 25.5 °C at 12:00 h to 28.7 °C at 23:00 h (Fig. 4b). As already shown in Fig. 2b for the daily means, in winter (July), the soil temperature was larger in 185 cm than in 15 cm depth, whereas in summer (December) the soil temperature was inverted compared to winter during all hours of the day (Figs. 4b, c).

In summer (December), the temperature difference across the 185 cm ranged between 11 and − 8 °C (Fig. 4f). The temperature difference between the soil in 15 cm depth and the air was 10–19 °C between 21:00 h and 9:00 h in December (Fig. 4d). In contrast, in July, the temperature difference between the soil in 15 cm depth and the air was only 4–6 °C between 23:00 h and 9:00 h, and the soil was colder than the air during the day (Fig. 4d). In Winter (July), the temperature difference between the soil in 185 cm depth and the air above the soil was positive throughout the day and ranged between 2 and 16 °C (Fig. 4f)

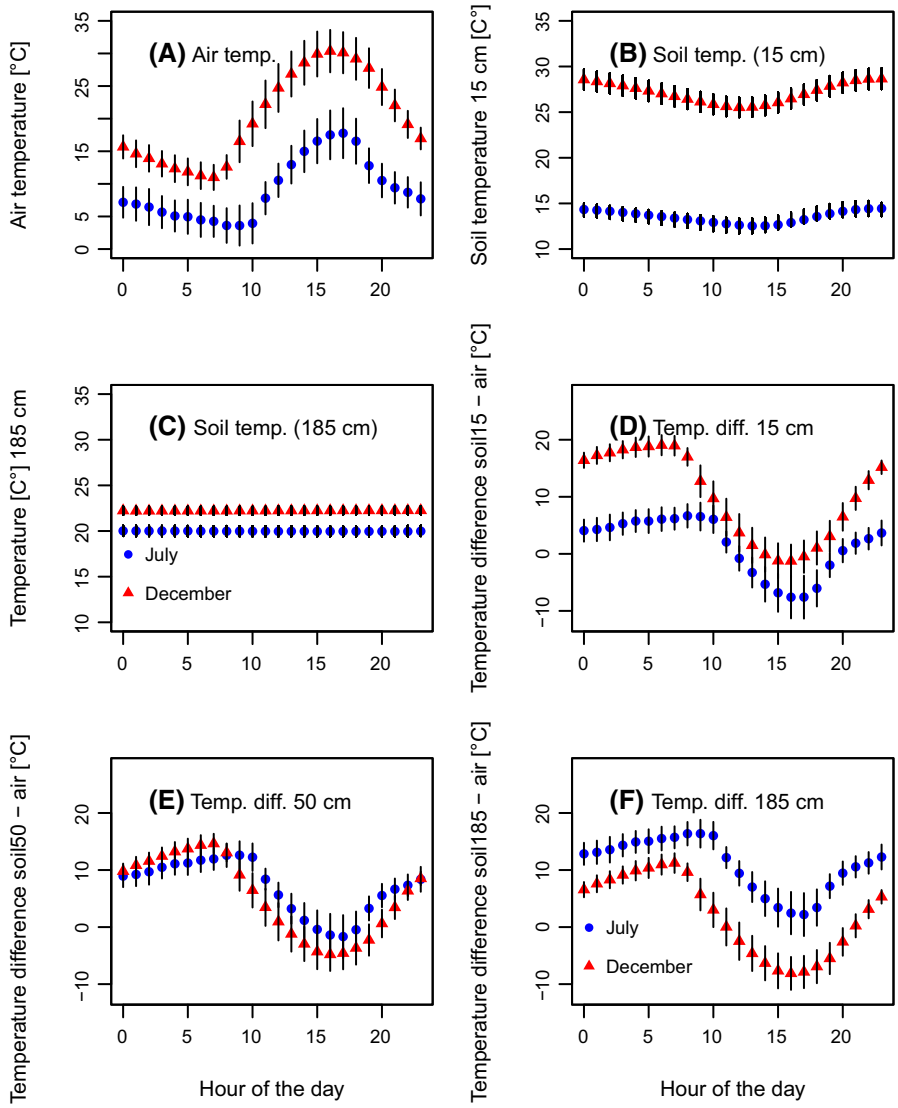

Fig. 4 Air temperature (**a**), soil temperature in 15 cm (**b**) and 185 cm (**c**) soil depth as well as the difference between soil temperature and air temperature for the uppermost 15 cm (**d**), 50 cm (**e**) and 185 cm (**f**) in July and December as a function of time of the day. Symbols indicate means, and arrows depict standard deviations calculated across all days of the two months in 2019 (n = 31). Please notice that the temperature differences are calculated as the soil temperature minus the air temperature

Considering the whole soil profile down to 185 cm (H = 1.85 m) in July, *Ra* increased during the night until 10:00 h in the morning (Fig. 5a). Assuming a permeability of 1×10^{-7} m^2, *Ra* reached Ra_c in the period between 4:00 and 10:00 h. At a permeability lower than 1×10^{-7} m^2, *Ra* remained below Ra_c throughout the day. In summer (December), the soil temperature decreased with increasing soil depth (Fig. 2b). Therefore, for December, we only calculated *Ra* for the upper 15 cm (H = 0.15 m), and found that a permeability of 1×10^{-6} m^2 or higher is required to reach a *Ra* larger than Ra_c during nighttime (Fig. 5b).

Hysteresis

When plotting the CO_2 concentration in 15 cm soil depth as a function of the soil temperature at 15 cm depth, a hysteresis loop was observed, both for July and December (Fig. 6). The hysteresis resulted from

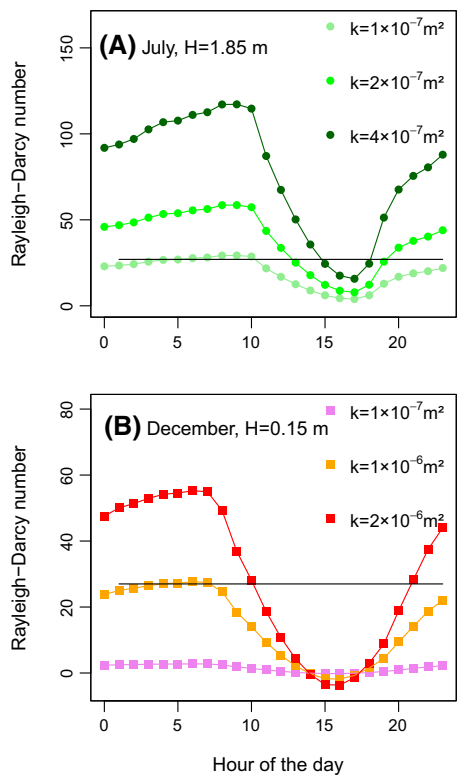

Fig. 5 Rayleigh-Darcy number as a function of time of the day for the upper 185 cm of the soil profile in July (**a**) and the upper 15 cm of the soil in December (**b**). The black horizontal line indicates the critical Rayleigh-Darcy number (Ra_c = 27)

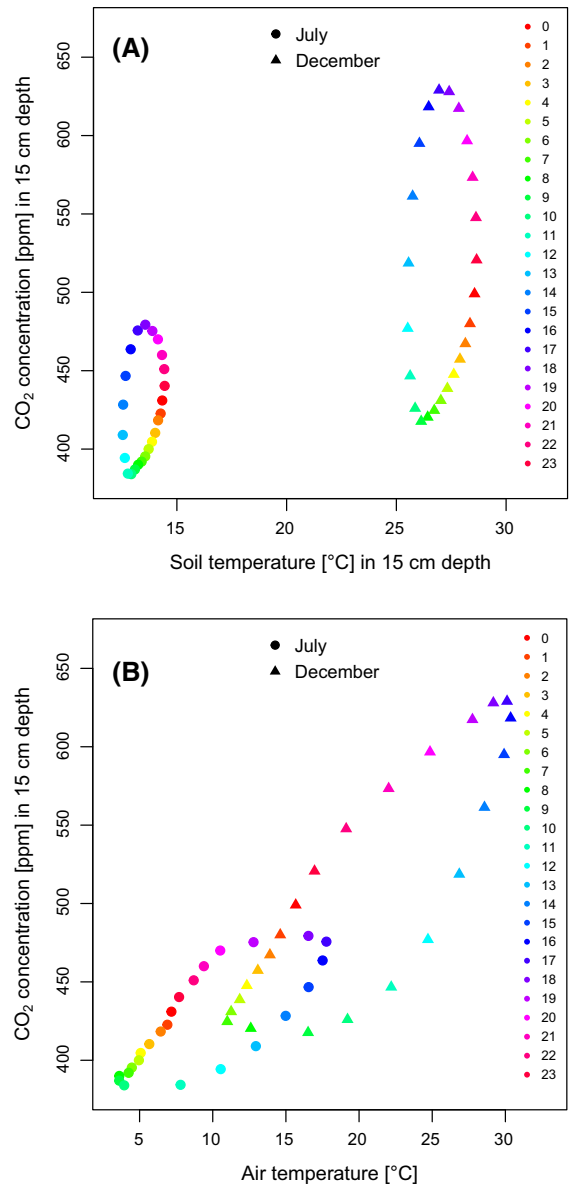

Fig. 6 CO_2 concentration in 15 cm soil depth as a function of soil temperate (**a**) and air temperature (**b**) in December and July 2019. Shown are hourly measurements calculated across all days of the month (n = 31) for December and July. Colors indicate the hour of the day

the fact that the CO_2 concentration was at its minimum in the morning, and reached its maximum in the late afternoon, while the soil temperature was at its minimum around noon and reached its maximum at 23:00 h (Fig. 6a). Another hysteresis loop was observed when plotting the CO_2 concentration in 15 cm soil depth as a function of the air temperature,

for both July and December (Fig. 6b). In contrast to the soil temperature that changed little during the day, air temperature changed to a similar extent as the soil CO_2 concentration (in 15 cm depth) over the course of the day (Fig. 6b).

The hysteresis loops of the soil temperature and the CO_2 concentration turn counterclockwise (Fig. 6a) and the hysteresis loops of the air temperature and the CO_2 concentration turn clockwise (Fig. 6b). The reason for this is that the soil CO_2 concentration in the topsoil had a similar dynamic as the air temperature (Fig. 6a), whereas it had time-shifted minima and maxima compared to the soil temperature in the topsoil over the course of the day (see also Figs. 3a, 4a, b).

CO_2 after precipitation event

On May 29, 4 mm precipitation occurred at the study site after there had been no precipitation event with more than 0.25 mm of precipitation for several months (Fig. 1 and Übernickel et al. (2020)). Following this precipitation event in May, increased CO_2 concentrations were observed at 15, 30, and 50 cm soil depths (Fig. 7a). The CO_2 concentration increased faster following the rain event in 15 cm depth than in 50 cm depth. The increase in the CO_2 concentration after the rain event was largest in 15 cm depth (115 ppm). The number of days over which the mean CO_2 concentration remained significantly elevated was 8 days in 15 cm depth and 9 days both in 30 and 50 cm depth (Fig. 7b). The daily oscillation of the CO_2 concentration described before (see Fig. 3) was still observed with the same amplitude after the precipitation event (Fig. 7a).

Discussion

The unique dataset of high frequency measurements of CO_2 and temperature at different depths in a coarse-textured desert soil presented here reveals strong diel oscillation of the CO_2 concentration that decreased with soil depth. The oscillation of the CO_2 concentration coincided with a strong diel variation of the air temperature, whereas the soil temperature, even in the topsoil, changed very little over the course of one day.

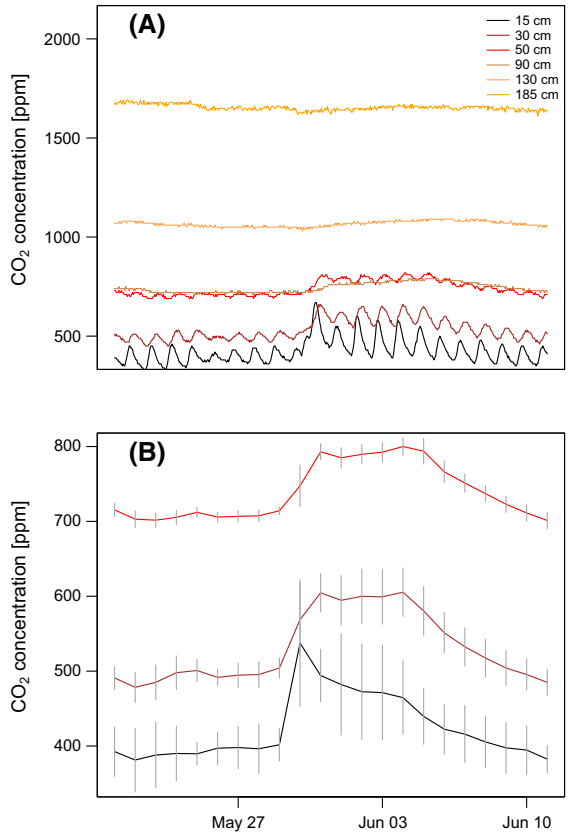

Fig. 7 Soil CO_2 concentrations in the time from May 21 to June 11, covering the rain event which took place on May 29. Hourly measured CO_2 concentrations in six different soil depths (**a**) and daily mean CO_2 concentrations and daily standard deviations (n = 24) in 15, 30 and 50 cm depth (**b**) are shown

Diel changes in CO_2 concentrations

The strong diel oscillation of the soil CO_2 concentration in the topsoil could be caused either by variation in the production of CO_2 in the soil or variation in the efflux of CO_2 from the soil. The soil CO_2 concentration changed by 95 to 211 ppm over the course of the day, while the soil temperature changed only by 2 °C during the same time (Fig. 6a). Given the small change in temperature, it is unlikely that such a strong change in the CO_2 concentration is caused by the temperature-dependence of the production of CO_2 by microorganisms or plant roots, as pointed out earlier by Ruehr et al. (2010) with respect to similar observations. We propose that the diel variation in the CO_2 concentration is caused by TCV leading to transport of CO_2-rich air from the soil to the atmosphere at night when the soil is substantially

warmer than the atmosphere (Fig. 4). Thermal convection has been shown to cause transport of CO_2 from soil when the soil has a high porosity and is warmer than the air by Ganot et al. (2014) based on column experiments.

In order to evaluate under which conditions TCV can occur in the soil under study, we calculated the Rayleigh-Darcy number (Fig. 5). In July, the soil temperature increased with increasing soil depths, and thus the soil depth over which the temperature gradient spans (H, see Eq. 1) is large. Given the large soil depth and the relatively large temperature differences between the subsoil and the air at night (Fig. 4), *Ra* values above Ra_c were reached at night and in the morning (Fig. 5a), indicating that TCV took place. The soil has high gravel and sand contents that increase with depth (Table 1), and thus a relatively high permeability. However, estimating the mean permeability over the whole soil profile is associated with a large uncertainty, which causes a large uncertainty in the *R*a estimate (Fig. 5). It also needs to be considered that the bedrock at the study soil is deeply weathered, and the upper meters of the saprolite have many fractures (Krone et al. 2021). Thus, the depth (H) over which conductive transport can take place is very likely several m, and not only 1.85 m as assumed here. If a larger H is considered, $Ra > Ra_c$ is reached also with smaller permeability (k). Finally, it needs to be taken into account that the soil profile is located on a hillslope (Fig. S1, Supplementary Information). For bodies with sloping boundaries, the conventional Rayleigh criterion is not directly applicable, and at slopes, TCV is much more likely to occur than on a plane, even in moderately permeable materials (Rose and Guo 1995; Nield and Bejan 2013).

At the second and third soil depth (30 and 50 cm), the CO_2 concentrations also underwent diel oscillation that was time-shifted compared to the topsoil (Fig. 3). The dynamic of the CO_2 concentration in the different depths of the soil can be explained by a convection cell model, where the different soil layers are different convection cells, and CO_2-rich air moves slowly from lower soil layers to upper soil layers due to thermal convection.

In summer (December), the soil temperature decreased with increasing soil depths, which does not favor TCV from the subsoil (Fig. 2a). This is likely the reason why soil CO_2 concentrations were larger in December than in July (Fig. 3). Still, even in December, the soil was much warmer than the air at night in all measured depths (Fig. 4d-f). Given the temperature gradient in the soil (Fig. 2b), TCV across the whole soil profile is not likely, but TCV from the upper cm of the soil might still occur. Therefore, we calculated *Ra* for December only over the upper 15 cm of the soil (Fig. 5b). The small H requires high permeability $\geq 1 \times 10^{-7}$ m^2 for *Ra* to exceed Ra_c (Fig. 5b), hence TCV to occur. It is questionable if the studied soil has such a high permeability. While the soil texture and gravel content (Table 1) indicate that the permeability is likely lower than 1×10^{-7} m^2 (Bear, 2013), it might still be that the many coarse stones in the topsoil (Fig. S1, Supplementary Information) facilitate gas transport along their surface. It might also be that small channels, created by insects or roots, increase the permeability of the soil and thus contribute to TCV of the soil. In addition, it can be speculated that numerous fractures in the upper m of the soil (Krone et al. 2021) which connect the subsoil with the atmosphere, might allow for nocturnal TCV to take place in December even against a temperature gradient in the topsoil, given that the subsoil was 10 °C warmer than the atmosphere at night (Fig. 4f). This has shown to be theoretically possible by Rose and Guo (1995). Finally, it needs to be taken into account that the soil profile is located on a hillslope (Fig. S1, Supplementary Information), where, the conventional Rayleigh criterion is not directly applicable, and TCV is much more likely to occur than on a plane, as mentioned above.

Furthermore, it needs to be considered that the oscillation of the soil CO_2 concentration can potentially also be caused by the radiation-dependence of plant root respiration (Carbone and Trumbore 2007). However, it seems rather unlikely that variation in photosynthetic activity alone caused the strong diel oscillation of the soil CO_2 concentration throughout the year, given the low precipitation (Fig. 1) and the sparse vegetation (see Sect. 2.1 and Fig. S1, Supplementary Information). Furthermore, radiation-dependent plant activity cannot explain why the CO_2 concentration was higher in December than in July, particularly given that plant activity was likely elevated in July after the rainfall (Figs. 1).

Taken together, the diel oscillation of the CO_2 concentration in the topsoil of this desert could be caused either by an oscillation of (1) the light- and soil temperature-dependent production of CO_2 by biota or

(2) the thermal convection of CO-rich air from the soil at night. Given the sparse vegetation, the low precipitation, and the large temperature differences between soil and air at night, the latter explanation seems more likely and it also explains the higher CO_2 concentrations in December than in July.

Rainfall increases CO_2 concentrations

We found the CO_2 concentration increased after only a few mm of precipitation (Fig. 6). The reason for this is likely that microorganisms in the desert soil react very sensitively to water inputs. This is supported by a laboratory study with topsoil from the study site showing that even small inputs of water that increased the soil water content to only 20% of the soil's water holding capacity, strongly increased the soil respiration (Seuss 2021). However, given that only 4 mm of rainfall caused an increase in the CO_2 concentration in 50 cm depth (Fig. 6), it seems likely that the increase in the CO_2 concentration was not only caused by microorganisms but at least partly also by root respiration, since the small amount of water likely did not reach a depth of 50 cm in the soil. Plants might have taken up water in the topsoil, which stimulated their activity leading to higher plant root respiration, also in a depth of 50 cm. This is supported by previous studies, showing that the soil CO_2 concentration is affected by precipitation through plant root respiration in desert soils (Wang et al. 2014; Song et al. 2015).

The total amount of rainfall during the study period was very low, which is related to the mega-drought Chile is currently experiencing (Morales et al. 2020). Rainfall at the study site can usually be observed in June. Yet, in June 2019, the amount of total respiration was lower compared to the three previous years (Übernickel et al. 2020). It can be assumed that in years in which the precipitation is higher at the study site, the soil CO_2 concentration is elevated due to increased biological activity.

Soil CO_2 in desert soils

The CO_2 concentrations measured here were relatively low throughout the year, and even at 185 cm depth did not exceed 1800 ppm. Besides low precipitation (see above), this can be attributed to the relatively low root density, low organic carbon content, and low microbial biomass (as indicated by the low DNA content), which cause low CO_2 production. In addition, the coarse texture (Table 1) allows for fast emission of CO_2, as discussed above. The low CO_2 concentration found here is in agreement with Amundson and Davidson (1990) who reported based on a literature survey that the lowest soil CO_2 concentrations across different ecosystems are typically observed in desert soils. Furthermore, Amundson et al. (1989) reported about a vegetation gradient in the eastern Mojave Desert that the lowest soil CO_2 concentrations in this gradient were found at a site that had the lowest vegetation density and the lowest soil TOC content. This site had a MAP of 160 mm and the soil CO_2 concentration in the upper 75 cm did not exceed 1000 ppm, which is similar to the site studied here. The low CO_2 concentrations observed here are also in accordance with Terhune and Harden (1991) who studied seasonal variations of CO_2 concentrations in stony, coarse-textured desert soils of southern Nevada, USA and observed that the CO_2 concentration in the upper 100 cm exceeded 1000 ppm only in spring. The authors attributed the relatively small soil CO_2 concentration to the coarse texture of the soils that allowed for fast transport of CO_2 from the soil to the atmosphere. Furthermore, the low CO_2 concentrations found here are in accordance with small CO_2 concentrations in two soils located at the southern margin of the Great Basin Desert in Nevada, USA, where MAP was 151 and 180 mm, respectively, and the CO_2 concentration measured over the whole year did not exceed 1000 ppm in the upper 100 cm of the soils (Oerter et al. 2018).

Throughout the year, the CO_2 concentration increased with soil depth despite the strong decrease in roots, TOC, and DNA with depth (Table 1). An increase in the CO_2 concentration with depth has been observed in many soils in different ecosystems (Solomon and Cerling 1987; Amundson et al. 1989; Castell and Galloway 1990; Richter and Markewitz 1995; Trumbore et al. 1995; Schwendenmann and Veldkamp 2006; Kim et al. 2017; Oerter et al. 2018). In the current study, the increase in the CO_2 concentration can likely be attributed to the fact that the air density increases with increasing CO_2 concentration, which leads to gravitational percolation of CO_2-rich air through soil pores towards deeper soil horizons (Kowalski and Sánchez-Cañete 2010; Sánchez-Cañete et al. 2013).

Conclusions

The unique dataset of high frequency measurements of CO_2 and temperature at different depths of a deep, coarse-textured desert soil presented here reveals diel oscillation of the CO_2 concentration and a hysteretic relationship between the soil CO_2 concentration and soil as well as air temperature, as hypothesized. The diel oscillation of the CO_2 concentration and the hysteretic relationship between soil CO_2 concentration and air temperature were very likely caused by thermal convection, leading to transport of CO_2-rich air from the soil to the atmosphere at night. Our results have important implications as they indicate that the soil CO_2 concentration can be strongly affected by the difference between soil and air temperature in soils. The results suggest that TCV might strongly contribute to gas exchange of soils, which is important for soil chemical reactions including weathering processes.

Acknowledgements We thank the German Research Foundation (DFG) for funding the project SP1389/5-2 in the frame of the priority research program SPP-1803 "EarthShape: Earth Surface Shaping by Biota". We thank the electronic workshop of the University of Bayreuth for technical support. We are grateful for access to the study site. We thank Andrea Scheibe und Carolin Waldemer for their help in the field and Renate Krauß and Uwe Hell for their help in the lab. We are grateful to Felipe Aburto's family for deinstalling the sensors and sending them back to Europe. We thank everyone involved in the installation and maintanence of the weather station.

Funding Open access funding provided by Swedish University of Agricultural Sciences. The study was funded by DFG (Grant SP1389/5–2).

Data availability The data are available in the Electronic Supplement of this contribution and at the BayEOS server (http://www.bayceer.uni-bayreuth.de/bayeos/en/bayeos-ser/gru/html.php?id_obj=107625), using the username and password "guest".

Declarations

Conflict of interest The authors declare no conflict of interest.

Code availability (software application or custom code) All code is available in the supplement.

References

Amundson RG, Davidson EA (1990) Carbon dioxide and nitrogenous gases in the soil atmosphere. J Geochem Explor 38(1–2):13–41

Amundson RG, Chadwick OA, Sowers JM (1989) A comparison of soil climate and biological activity along an elevation gradient in the eastern Mojave Desert. Oecologia 80(3):395–400

Bear J (2013) Dynamics of fluids in porous media. Courier Corporation

Bernhard N, Moskwa LM, Schmidt K, Oeser RA, Aburto F, Bader MY, Brucker E, Kühn P (2018) Pedogenic and microbial interrelations to regional climate and local topography: new insights from a climate gradient (arid to humid) along the Coastal Cordillera of Chile. CATENA 170:335–355

Brucker E, Spohn M (2019) Formation of soil phosphorus fractions along a climate and vegetation gradient in the Coastal Cordillera of Chile. CATENA 180:203–211

Burt R (2004) Soil survey laboratory methods manual V4.0, United States Department of Agriculture, Lincon, Nebraska

Carbone MS, Trumbore SE (2007) Contribution of new photosynthetic assimilates to respiration by perennial grasses and shrubs: residence times and allocation patterns. New Phytol 176(1):124–135

Côté J, Fillion MH, Konrad JM (2011) Intrinsic permeability of materials ranging from sand to rock-fill using natural air convection tests. Can Geotech J 48(5):679–690

Flechard CR, Neftel A, Jocher M, Ammann C, Leifeld J, Fuhrer J (2007) Temporal changes in soil pore space CO_2 concentration and storage under permanent grassland. Agric for Meteorol 142(1):66–84

Ganot Y, Dragila MI, Weisbrod N (2014) Impact of thermal convection on CO_2 flux across the earth–atmosphere boundary in high-permeability soils. Agric for Meteorol 184:12–24

Gaumont-Guay D, Black TA, Griffis TJ, Barr AG, Jassal RS, Nesic Z (2006) Interpreting the dependence of soil respiration on soil temperature and water content in a boreal aspen stand. Agric for Meteorol 140(1–4):220–235

Jassal R, Black A, Novak M, Morgenstern K, Nesic Z, Gaumont-Guay D (2005) Relationship between soil CO_2 concentrations and forest-floor CO_2 effluxes. Agric for Meteorol 130(3–4):176–192

Jia X, Zha T, Wu B, Zhang Y, Chen W, Wang X, He G (2013) Temperature response of soil respiration in a Chinese pine plantation: hysteresis and seasonal vs. diel Q 10. PLoS one 8(2):e57858

Kämpf H, Bräuer K, Schumann J, Hahne K, Strauch G (2013) CO_2 discharge in an active, non-volcanic continental rift area (Czech Republic): characterisation (δ13C, 3He/4He) and quantification of diffuse and vent CO_2 emissions. Chem Geol 339:71–83

Kim H, Stinchcomb G, Brantley SL (2017) Feedbacks among O_2 and CO_2 in deep soil gas, oxidation of ferrous minerals, and fractures: A hypothesis for steady-state regolith thickness. Earth Planet Sci Lett 460:29–40

Kowalski AS, Sánchez-Cañete EP (2010) A new definition of the virtual temperature, valid for the atmosphere and the CO_2-rich air of the vadose zone. J Appl Meteorol Climatol 49(8):1692–1695

Krone LV, Hampl FJ, Schwerdhelm C, Bryce C, Ganzert L, Kitte A, von Blanckenburg F (2021) Deep weathering in the semi-arid Coastal Cordillera, Chile. Sci Rep 11(1):1–15

Laemmel T, Mohr M, Longdoz B, Schack-Kirchner H, Lang F, Schindler D, Maier M (2019) From above the forest into the soil – how wind affects soil gas transport through air pressure fluctuations. Agric Meteorol 265:424–434

Levintal E, Dragila MI, Kamai T, Weisbrod N (2017) Free and forced gas convection in highly permeable, dry porous media. Agric Meteorol 232:469–478

Maier M, Schack-Kirchner H, Aubinet M, Goffin S, Longdoz B, Parent F (2012) Turbulence effect on gas transport in three contrasting forest soils. Soil Sci Soc Am J 76(5):1518–1528

Min K, Berhe AA, Khoi CM, van Asperen H, Gillabel J, Six J (2020) Differential effects of wetting and drying on soil CO2 concentration and flux in near-surface vs deep soil layers. Biogeochemistry 148(3):255–269

Morales MS, Cook ER, Barichivich J, Christie DA, Villalba R, LeQuesne C, Matskovsky V (2020) Six hundred years of South American tree rings reveal an increase in severe hydroclimatic events since mid-20th century. Proc Natl Acad Sci 117(29):16816–16823

Moya MR, Sánchez-Cañete EP, Vargas R, López-Ballesteros A, Oyonarte C, Kowalski AS, Serrano-Ortiz P, Domingo F (2019) CO_2 dynamics are strongly influenced by low frequency atmospheric pressure changes in semiarid grasslands. J Geophys Res Biogeosci 124(4):902–917

Moyano FE, Manzoni S, Chenu C (2013) Responses of soil heterotrophic respiration to moisture availability: An exploration of processes and models. Soil Biol Biochem 59:72–85

Nachshon U, Weisbrod N, Dragila MI, Ganot Y (2011) The importance of advective fluxes to gas transport across the earth-atmosphere interface: the role of thermal convection. Planet Earth 2011: Global Warming Challenges and Opportunities for Policy and Practice 353

Nield DA, Bejan A (2013) Convection in porous media, vol 3. Springer, New York.

Noy-Meir I (1973) Desert ecosystems: environment and producers. Annu Rev Ecol Syst 4(1):25–51

Oerter E, Mills JV, Maurer GE, Lammers LN, Amundson R (2018) Greenhouse gas production and transport in desert soils of the Southwestern United States. Global Biogeochem Cycles 32(11):1703–1717

Oeser RA, Stroncik N, Moskwa LM, Bernhard N, Schaller M, Canessa R, Fuentes JP (2018) Chemistry and microbiology of the Critical Zone along a steep climate and vegetation gradient in the Chilean Coastal Cordillera. CATENA 170:183–203

Parkin TB, Kaspar TC (2003) Temperature controls on diurnal carbon dioxide flux. Soil Sci Soc Am J 67(6):1763–1772

Phillips CL, Nickerson N, Risk D, Bond BJ (2011) Interpreting diel hysteresis between soil respiration and temperature. Glob Change Biol 17(1):515–527

R Core Team (2018). R: A language and environment for statistical computing. R Foundation for Statistical Computing. http://www.R-project.org/, Vienna, Austria

Ramnarine R, Wagner-Riddle C, Dunfield KE, Voroney RP (2012) Contributions of carbonates to soil CO_2 emissions. Can J Soil Sci 92(4):599–607

Rey A (2015) Mind the gap: non-biological processes contributing to soil CO_2 efflux. Glob Change Biol 21(5):1752–1761

Ribando RJ, Torrance KE (1976) Natural convection in a porous medium: effects of confinement, variable permeability, and thermal boundary conditions. J Heat Transfer 98(1):42–48

Richter DD, Markewitz D (1995) How deep is soil? Bioscience 45(9):600–609

Riveros-Iregui DA, Emanuel RE, Muth DJ, McGlynn BL, Epstein HE, Welsch DL, Wraith JM (2007) Diurnal hysteresis between soil CO_2 and soil temperature is controlled by soil water content. Geophys Res Lett 34(17)

Roland M, Vicca S, Bahn M, Ladreiter-Knauss T, Schmitt M, Janssens IA (2015) Importance of nondiffusive transport for soil CO_2 efflux in a temperate mountain grassland. J Geophys Res Biogeosci 120(3):502–512

Rose AW, Guo W (1995) Thermal convection of soil air on hillsides. Environ Geol 25(4):258–262

Ruehr NK, Knohl A, Buchmann N (2010) Environmental variables controlling soil respiration on diurnal, seasonal and annual time-scales in a mixed mountain forest in Switzerland. Biogeochemistry 98(1–3):153–170

Sánchez-Cañete EP, Kowalski AS, Serrano-Ortiz P, Pérez-Priego O, Domingo Poveda F (2013) Deep CO_2 soil inhalation/exhalation induced by synoptic pressure changes and atmospheric tides in a carbonated semiarid steppe. Biogeosciences 10:6591–6600

Sandaa RA, Enger Ø, Torsvik V (1998) Rapid method for fluorometric quantification of DNA in soil. Soil Biol Biochem 30(2):265–268

Schimel JP (2018) Life in dry soils: effects of drought on soil microbial communities and processes. Annu Rev Ecol Evol Syst 49:409–432

Schimel DS, House JI, Hibbard KA, Bousquet P, Ciais P, Peylin P, Canadell J (2001) Recent patterns and mechanisms of carbon exchange by terrestrial ecosystems. Nature 414(6860):169–172

Schwendenmann L, Veldkamp E (2006) Long-term CO_2 production from deeply weathered soils of a tropical rain forest: evidence for a potential positive feedback to climate warming. Glob Change Biol 12(10):1878–1893

Seuss I (2021) Microbial processes depending on soil water content in soils along a climate gradient in Chile. Master

thesis in Geoecology. University of Bayreuth (the thesis was submitted on March 24, 2021; Main supervisor: M. Spohn)

Solomon DK, Cerling TE (1987) The annual carbon dioxide cycle in a montane soil: observations, modeling, and implications for weathering. Water Resour Res 23(12):2257–2265

Song W, Chen S, Zhou Y, Wu B, Zhu Y, Lu Q, Lin G (2015) Contrasting diel hysteresis between soil autotrophic and heterotrophic respiration in a desert ecosystem under different rainfall scenarios. Sci Rep 5:16779

Spohn M, Klaus K, Wanek W, Richter A (2016) Microbial carbon use efficiency and biomass turnover times depending on soil depth–Implications for carbon cycling. Soil Biol Biochem 96:74–81

Takle ES, Massman WJ, Brandle JR, Schmidt RA, Zhou X, Litvina IV, Rice CW (2004) Influence of high-frequency ambient pressure pumping on carbon dioxide efflux from soil. Agric for Meteorol 124(3–4):193–206

Tan KK, Sam T, Jamaludin H (2003) The onset of transient convection in bottom heated porous media. Int J Heat Mass Transf 46(15):2857–2873

Terhune CL, Harden JW (1991) Seasonal variations of carbon dioxide concentrations in stony, coarse-textured desert soils of southern Nevada, USA. Soil Sci 151(6):417–429

Trumbore SE, Davidson EA, Barbosa de Camargo P, Nepstad DC, Martinelli LA (1995) Belowground cycling of carbon in forests and pastures of Eastern Amazonia. Global Biogeochem Cycles 9(4):515–528

Übernickel K, Ehlers TA, Ershadi MR, Paulino L, Fuentes Espoz J-P, Maldonado JP, Oses-Pedraza R, von Blanckenburg F (2020) Time series of meteorological station data in the EarthShape study areas of the Coastal Cordillera. GFZ Data Services, Chile. https://doi.org/10.5880/fidgeo.2020.043

Vázquez M, Ramírez S, Morata D, Reich M, Braun JJ, Carretier S (2016) Regolith production and chemical weathering of granitic rocks in central Chile. Chem Geol 446:87–98

Wang B, Zha TS, Jia X, Wu B, Zhang YQ, Qin SG (2014) Soil moisture modifies the response of soil respiration to temperature in a desert shrub ecosystem. Biogeosciences 11(2):259

Weisbrod N, Dragila MI, Nachshon U, Pillersdorf M (2009) Falling through the cracks: the role of fractures in Earth-atmosphere gas exchange. Geophys Res Lett 36(2)

Wood BD, Keller CK, Johnstone DL (1993) In situ measurement of microbial activity and controls on microbial CO2 production in the unsaturated zone. Water Resour Res 29(3):647–659

Zhang Q, Katul GG, Oren R, Daly E, Manzoni S, Yang D (2015) The hysteresis response of soil CO_2 concentration and soil respiration to soil temperature. J Geophys Res Biogeosci 120(8):1605–2161